**Keywords**

Magmatic Heat Budget,  
Hot Dry Rocks,  
Hot Wet Rocks  
South America,  
Geothermal Resources.

Received: January 30, 2019

Accepted: February 25, 2019

Published: March 25, 2019

# Assessment of Geothermal Resources of South America - A New Look

Fabio Vieira<sup>1</sup>, Valiya Hamza<sup>1</sup>,<sup>1</sup> Department of Geophysics, National Observatory, Rio de Janeiro, Brazil**Email address**

fabiovieira@on.br (F. Vieira)

Corresponding authors

**Abstract**

The present work provides a new look into the nature and distribution of geothermal resources of South America, on the basis of recent advances in data analysis and regional assessments. Notable in this context is the progress achieved in the use of a procedure termed as magmatic heat budget (MHB) that allow estimation of heat flux in areas of recent volcanic activity. In addition, an updated compilation of temperature gradients and heat flux have been completed. Such advances have allowed new resource assessments for 6526 sites. These span over more than 100 crustal blocks, distributed in thirteen countries of the continent. Following this, a 2°x2° grid system with homogenized data sets were employed for calculating the in-situ heat content. Determinations of resource base based on observational data are now available for 253 out of a total of 418 cells in this grid system. Values of resource base based on estimated heat flow were calculated for the remaining 165 grid elements. The data and model results on temperatures of subsurface strata at depths less than three kilometers have been employed in classifying the resources, into three general categories: hot dry rock (HDR), hot wet rock (HWR) and low enthalpy (LE). HDR type resources, classified as those with temperatures higher than 150°C, occur in 318 localities mainly in the Andean regions. Similarly, HWR type resources, classified as those with temperatures in the range of 90 to 150°C, occur in 352 localities. Low enthalpy (LE) resources, with temperatures < 90°C, are numerous mainly in the eastern parts of the continent. The total resource base (RB) of HDR systems is estimated to be 1329x10<sup>21</sup>J and the corresponding resource base per unit area (RBUA) is 513GJ/m<sup>2</sup>. The HWR systems have a total resource base of 586x10<sup>21</sup>J, while the corresponding value for RBUA is 409GJ/m<sup>2</sup>. The low enthalpy systems, with temperatures in the range of 60 to 90°C, have a total resource base of 240GJ/m<sup>2</sup>, while those with temperatures less than 60°C is estimated to be 210GJ/m<sup>2</sup>.

**1. Introduction**

Compilation of data sets on subsurface temperatures, heat flux, thermal spring discharges and geotectonic characteristics of subsurface strata constitute essential steps in assessments of geothermal resources. Evaluations of geothermal resources on global scale have been reported by Hutterer (2001), Lund and Freeston (2001) and Barbier (2002), among others. In the past few decades, several attempts have also been made in assessments of geothermal resources of South American continent (Battocletti, 1999; Cardoso et al, 2010; Vieira and Hamza, 2014). Results of regional assessments have also been reported on local scales for specific sub-regions of South America. Most of such works have been carried out as parts of updates of geothermal projects in Argentina (Miranda and Pesce, 1997; Pesce, 1995; 2000; 2005; Sigismondi, 2012), Bolivia (Delgadillo, 1997), Brazil (Hamza et al, 1978; Hamza and Eston, 1983; Eston and Hamza (1984); Hamza et al, 1990;

2005; 2010), Chile (Lahsen, 1988; Lahsen et al, 2005), Colombia (Alfaro et al, 2000; 2011), Ecuador (Almeida, 1988; Beate and Salgado, 2005; 2010), Peru (Parodi, 1975; Diaz and Guillermo, 1988) and Venezuela (Urbani, 1987; Almandoz and Rojas, 1988).

The resource estimates in much of these earlier studies made use of information concerning near surface geothermal manifestations and subsurface temperature data. This approach implies variable degrees of spatial resolution which is a major problem in assessments of resources in regions of low data density. Cardoso et al (2010) and Vieira and Hamza (2014) adopted a hybrid approach in which crustal structure and geothermal data were averaged over grid elements. Results of this hybrid approach has provided better insights into the assessments of geothermal resources on regional scales. A major weak point of the previous works has been the absence of resource assessments for areas of recent volcanic activity, a consequence of the lack of a suitable procedure for

estimating deep crustal heat flux in magmatic provinces. In the present work, a procedure, based on considerations of magmatic heat budget (MHB), has been introduced for estimating deep crustal heat flow in areas of recent volcanic activity. This approach has led to considerable improvements in assessments of resources of the type classified as hot dry rock (HDR) and hot wet rock (HWR), improving thereby reliability of resource estimates in areas of magma intrusions.

## 2. Geologic Context

The occurrence and distribution of geothermal resources in South American continent is intimately related to its geologic framework. The western side of this continent is known to host large number of localities with notable volcanic activities. The geologic context of such magmatic activities has been discussed in detail for the region of Western Sierras Pampeanas of Argentina by Rapela et al (2010), for cordilleran regions in Peru by Myers (1975) and orogenic systems in central-northern Ecuador by Guillier et al (2001). On the other hand, the interior parts of the continent are composed of low-lying platform areas which are tectonically quiescent and where basement rocks are of Precambrian to Proterozoic in age. It also hosts a large number of intracratonic basins. Some regions on the eastern parts are affected by alkaline intrusions of Tertiary age, but active volcanism is absent. Figure 1 provides a simplified view of the age provinces of the south American region.

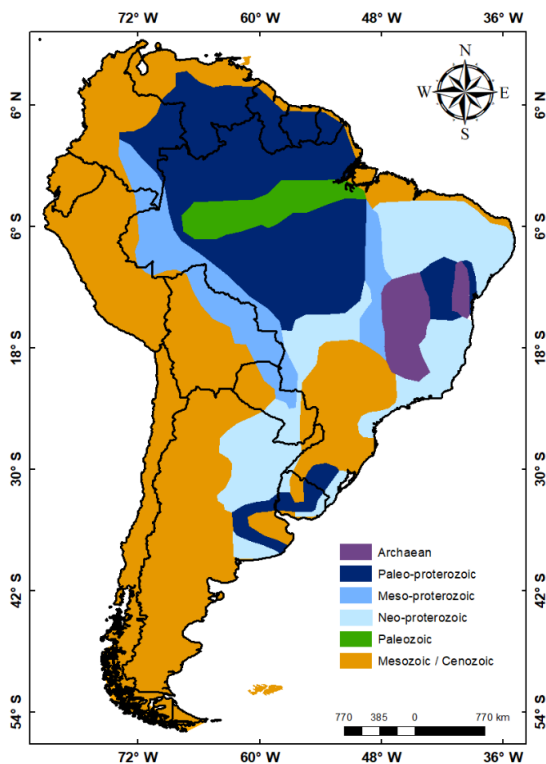


Figure 1 – Digital representation of age provinces in South America (Adapted from Vieira and Hamza, 2014).

## 3. Characteristics of Data Base

Geothermal data have been acquired, over the last few decades, at a number of localities in the South American continent. Summaries of such data sets have been reported by Hamza and Munoz (1996), Hamza et al (2005) and Vieira and

Hamza (2014). A number of different methods have been employed in determinations of geothermal gradients and heat flux. In accordance with the practice adopted in earlier publications (see for example, Hamza and Munoz, 1996) these methods are identified by three-letter abbreviations for determining geothermal gradients. Thus, the conventional method, designated by the abbreviation CVL, has been used in referring to the procedure employed for calculating geothermal gradients derived from results of incremental temperature logs of undisturbed boreholes (Beck, 1965). Similarly, the procedure used for determining gradients based on measurements in underground mine galleries (Bullard, 1939) has been identified by the abbreviation MGT. The BHT method refers to gradient values derived from bottom-hole temperature measurements carried out by oil industry in exploration wells (Carvalho and Vacquier, 1977). The CBT method is a variant of the BHT method, used for determining gradient values based on measurements of stable temperatures in undisturbed sections at the bottom parts of boreholes (Gomes and Hamza, 2005). Similarly, AQT method refers to a procedure developed for determining temperature gradients in flowing wells (Santos et al, 1986). Estimates of heat flux at sites of thermal springs have also been made making use of methods, designated as geochemical (GCL), which are variations of the procedures proposed initially by (Swanberg and Morgan, 1978; Hurter, 1986).

In the present work, it was found convenient to introduce some modifications in the designations of the methods used and also in its implementation, in previous publications. Thus, CVL (abbreviation for Conventional) has been renamed as ITL (abbreviation for Incremental Temperature Log) and CBT (abbreviation for Conventional Bottom Temperature) has been changed to the more appropriate SBT (meaning Stable Bottom Temperature). Also, complementary procedures were introduced in the application of the GCL method, details of which are provided in section (3.1). A major innovation of the present work has been introduction of a procedure for estimating heat flux for areas of recent volcanic activity. It has been designated as the method of magmatic heat budget (MHB). Details of MHB method are provided in section (3.2).

### 3.1. Modifications in the GCL method

In proposing the GCL method, Swanberg and Morgan (1978) adopted 13°C as the value for surface temperature in the equation for silica heat flow method. This value is indeed representative for western USA, but not necessarily valid for regions in South America. In the present work, use was made of ground surface temperature values reported in local meteorological records, in calculating heat flux by the GCL method.

Alexandrino and Hamza (2018) pointed out that the quality of statistical fits between temperatures and silica concentrations can be improved by considering a segmented approach. In this case, the solubility data is subdivided into separate sections and specific empirical relations developed for each section. In the present work, the lowermost limit for silica concentrations was set at 6.1 ppm. The upper limits considered for the four classes of silica concentrations are 47.4, 199.8, 595.3 and 763.6 ppm. The overall relation for these intervals may be written as:

$$T_{SiQ}(SiQ) = A + B.(SiQ) + C.(SiQ)^2 + D.\ln(SiQ) \quad (1)$$

where  $\text{SiO}_2$  is the concentration of silica in ppm and  $T_{\text{SiO}_2}$  the reservoir temperature in °C. The values of the constants A, B, C and D, provided in Table 1, were adopted in the present work.

Table 1 - Values of constants (cons) in equation 1 for four ranges of concentrations of silica.

Cons.	Range of dissolved silica (ppm)			
	6.1 – 47	47 - 200	200 – 595	595 -764
A	-41.85	-52.28	-119.05	-28001.00
B	0.33	0.20	0.05	-17.44
C	-6.70E-04	-1.10E-04	6.19E-05	6.88E-03
D	33.09	37.04	53.95	5669.77

Another modification adopted concerns use of the value for dissolved silica in thermal waters, which is essential in calculation of heat flux by the GCL method. In many localities, availability of data on dissolved silica was found to be limited, even though corresponding data for Na-K-Ca thermometry are available. There are also data sets where both silica and Na-K-Ca data has been acquired. In these latter cases, it has been possible to examine the relation between reservoir temperatures based on Na-K-Ca geothermometer with that obtained using silica thermometry. The results point to reasonably good correlations between values obtained by these two geochemical techniques. This correlation was used for calculating silica temperatures which were subsequently employed in determination of heat flux by the GCL method. An example of the relation obtained for central cordilleran region of Peru is presented in Figure 2.

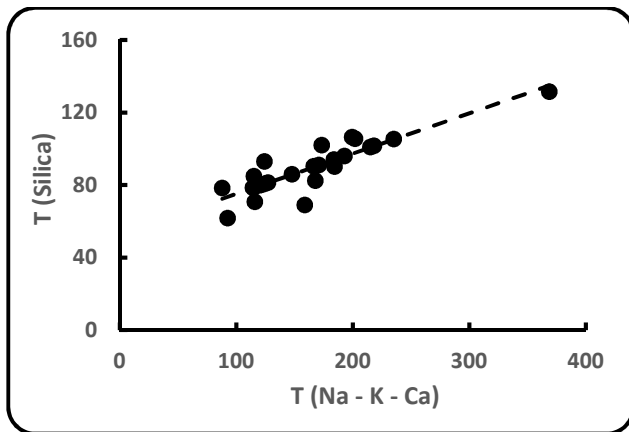


Figure 2 - Correlation between temperatures calculated using Na-K-Ca and Silica thermometric methods, for sites in northern Peru.

### 3.2. Heat Flux in Areas of Recent Volcanic Activity

Andean cordilleras are characterized by widespread volcanic activity and hold prospects for development of hot dry rock (HDR) projects. Geological models suggest the possibility that andesitic magma may underlie much of the localities of volcanic activity. This is significant because HDR reservoirs could potentially be sited in such areas. However, lack of suitable geothermal data has been a major obstacle in estimating deep crustal heat flux, which is a basic parameter in assessment of geothermal resources. It is in this context that attempts were made for developing a method for estimation of heat flux in areas of volcanic activities.

The essence of this new procedure, designated as the method of Magmatic Heat Budget – MHB, may be understood by considering the importance of residual heat in magma emplacement. In general, the quantity of residual heat is dependent on the magma volume emplaced and time elapsed after its emplacement. Smith and Shaw (1975) considered the relation between magma volume (in cubic kilometers) and time elapsed (in years) as approximately linear, when both are expressed on log scale. In the case of South America, it is convenient to examine the nature of such relations separately for the eastern and western parts of the continent. According to the available information (see for example: Silva and Francis, 1991; Stern, 2004) most of the recent volcanic activities in cordilleran regions have age values less than a few million years and the volumes of magma chambers emplaced are estimated to be in the range of  $10^4$  to  $10^7$   $\text{km}^3$ . Such information has been useful in evaluating areas with potential for development of high-temperature geothermal resources in South America. An example of this line of reasoning is illustrated in Figure 3 where the domain limited by dashed lines may be considered as representing the division between regions with and without residual magmatic heat. In other words, sites falling in the region below the belt of dashed lines may be considered as having potential for retaining residual magmatic heat in subsurface layers. For the same reason, sites falling above the belt of dashed lines may be considered as those with little residual magmatic heat.

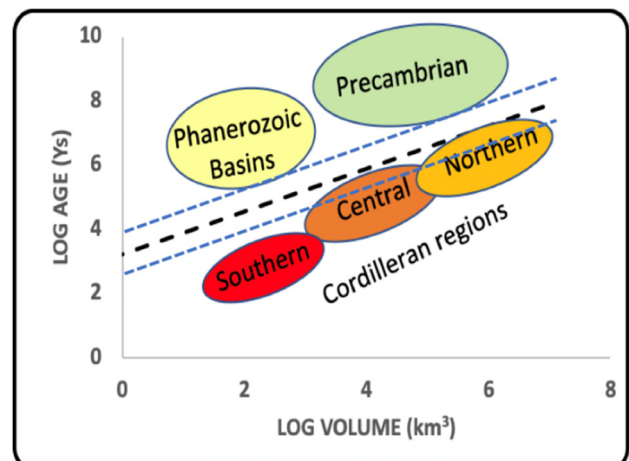


Figure 3 - Relation between magma volume and elapsed time of volcanic activity for the South American continent.

The next step in implementing the method of MHB is to look into suitable procedures for calculation of subsurface temperatures and heat flux. According to Noguchi (1970), Annen et al (2006) and Suarez (2017) the emplacement temperature of andesitic magma at mid crustal levels is approximately  $1200^\circ\text{C}$  while the depth of emplacement falls in the range of 5 to 15 km. Similar estimates were also made by Mamani et al (2000) and Borzotta et al (2018). For the purposes of the present work a representative depth of  $12.5 \pm 5$  km has been assumed for all areas of recent volcanism in the Andean region. This is obviously a first order simplification, which can be improved with availability of more reliable data. Noguchi (1970) argued that magma temperatures drops to about  $900^\circ\text{C}$  in about 60000 years after emplacement. This allows intra-crustal magma chamber emplacement temperature ( $T_{\text{emp}}$ ) to be estimated for the time interval of

emplacement ( $a_{emp}$ ). For the age range of 0 to 60000 years, the relation is:

$$T_{emp} = 1200 - (300/60000) a_{emp} \quad (2)$$

The next step in the MHB method is determination of heat flux corresponding to the emplacement temperature  $T_{emp}$ . For a crust with temperature dependent thermal conductivity ( $\lambda$ ) the relevant relation for magmatic heat flux ( $q_{emp}$ ) corresponding to residual temperature  $T_{emp}$  as a function of depth ( $z$ ) is (Carslaw and Jaeger, 1959; Hamza, 1982):

$$q_e(z) = \frac{\lambda_0}{z_s \alpha} \ln\left(\frac{\theta_m}{\theta_0}\right) \quad (3)$$

where  $\theta_m = 1 + \alpha T_{emp}$  and  $\theta_0 = 1 + \alpha T_0$ ,  $\alpha$  being the temperature coefficient of thermal conductivity and  $T_0$  the surface temperature. The subscript zero indicate values of parameters evaluated at the surface ( $z = 0$ ). Note that we have ignored the contribution of radiogenic heat, as it is only of secondary importance in the present context. For values of time elapsed larger than 60000 years it is assumed that the emplacement temperature magma drops to about 500°C at the depth of 12.5km, which imply a heat flux of 80mW/m<sup>2</sup>. The limitations in the arguments of Noguchi (1970) and Smith and Shaw (1975) impose constraints on calculations by equation (2). Thus, heat flux values obtained using MHB method should be considered as first order approximations, useful for assessment of resources in areas of recent magmatic activity. On the other hand, such limitations are considered to be of relatively minor importance in the present context of resource estimates for deep crustal strata. Hence data acquired using MHB method may be considered as capable of providing reasonably reliable estimates of deep crustal resources.

MHB method has been employed for deriving estimates of heat flux in areas of recent volcanism in Argentina, Bolivia, Brazil, Chile, Colombia, Ecuador and Peru. However, reliable age data, necessary for estimation of heat flux by the MHB method, were available for only 272 localities. Chile stands out as the country with the largest number of volcanic areas, followed by Argentina, Bolivia and Peru. Examples of the parameter values adopted in MHB method for selected volcanic areas are provided in Table 2.

Table 2 - Examples of parameter values adopted in MHB method for selected areas of recent volcanism in South America.

( $a_{emp}$  – Elapsed time since magma emplacement;  $D_m$  – Depth of magma chamber;  $T_m$  – Temperature of magma chamber;  $q$  – heat flux in mW/m<sup>2</sup>).

Volcanic Area	$a_{emp}$ (Ys)	$D_m$ (km)	$T_m$ (°C)	$q$ (mW/m <sup>2</sup> )
Copahue (ARG)	25	< 2	1190	160
Chascon (BOL)	8800	12.5	760	80
Jayu Outa (BOL)	60000	12.5	900	130
Tacora (CHI)	5980	<5	~ 1170	160
Azufra (COL)	<10	<5	~ 1195	160
Cotopaxi (ECU)	<5	<5	1200	160
Ampato (PER)	60000	~ 10	900	80
Cabugi (BRA)	1900000	~15	500	70

#### 4. Overview of Heat Flux Data Sets

According to the compilation of the present work heat flux values relevant for resource assessments are available for 6526 localities in South American continent. These sites are distributed in ten out of thirteen countries in the continent. Table 3 provides a summary of the methods used for geothermal data in 13 countries of South America. There is a total of 6534 heat flux values. The country codes (ID) in the first column of this table are: ARG – Argentina; BOL – Bolivia; BRA – Brazil; CHI – Chile; COL – Colombia; ECU – Ecuador; FGU – French Guiana; GUY – Guyana; PAR – Paraguay; PER – Peru; SUR – Suriname; URU – Uruguay; VEN – Venezuela.

As can be verified from data in this table, most of the heat flux values for South America have been obtained using BHT and the closely related SBT methods (5337 values). Some regions have relatively high data density, as in the case of Magdalena valleys in central parts of Colombia, Neuquén basin in Argentina and areas of thermal springs in the southeastern cordillera of Peru. The high data densities in Colombia and Argentina arise from the large number of heat flux values derived using BHT data in closely spaced oil wells. The high data density in southeast cordilleran region of Peru indicate heat flux values derived for areas of thermal springs using the GCL method. Marine heat flux method (OHF) has been used for heat flux measurements in Lake Titicaca, Peru (Sclater et al, 1970) and Lago General Carrera and Lago Cochrane, southern Chile (Murdie et al, 1999). With large areas of recent volcanic activities, Chile has the largest number of heat flux values derived using the MHB method. Heat flux data are available for 150 localities in Bolivia, the majority have been acquired using BHT, GCL and MHB methods. In the case of Venezuela, the values reported are those derived using the GCL methods. Most of the heat flux data in Brazil are derived using ITL, BHT and SBT methods. In the case of Paraguay, BHT method was used for data acquisition for sites in the Chaco-Pampa basin system. Heat flux in Uruguay has been estimated using the AQT method for 7 localities. Suitable thermal gradient and heat flow data are not available for Guyana, French Guiana, Suriname and Trinidad.

Table 3 - Summary heat flux data for ten countries of the South American continent. ID – country code. For details see text. (\* The number of ITL data for Peru and Chile include results of measurements in lakes, using marine heat flux techniques - OHF).

ID	Number of localities with heat flux determinations						
	ITL	MGT	BHT	SBT	AQT	GCL	MHB
ARG	4		165		6	197	64
BOL	11	9	32			43	55
BRA	109	2	297	302	41	72	2
CHI	22*		1	6		35	72
COL	3		4407			36	16
ECU	1		40			18	32
FGU							
GUY							
PAR			35				
PER	32*	3	52		1	234	30
SUR							
URU					7		
VEN						40	
Total	182	14	5029	308	55	675	271

## 5. Gridding and Homogenization

The summary of heat flux measurements in Table 3 reveals considerable variations in data density. Such variations are inconvenient features in deriving maps and also in regional assessment of geothermal resources. Clearly, there is need for homogenization of data sets. In the present work, a  $2^\circ \times 2^\circ$  grid system was adopted for setting up the area elements, for which mean values could be calculated. This choice grid system was considered reasonable, taking into account the characteristics of data set. Smaller grid systems were considered undesirable in view of the low data density, while larger ones were found to lead to excessive smoothing of regional variations in heat flux.

In essence mean of experimental heat flux values are assigned to those area elements for which observational data are available. Following this, estimated values of heat flux, based on empirical heat flow-age relation (Hamza and Verma, 1969) are assigned to area elements for which observational data are not available. The grid system adopted in the present work consists of a total of 418 cells, out of which 253 have been assigned mean heat flow values derived on the basis of observational data. Estimated heat flux values, derived from the empirical heat flow-age relation, were assigned to the remaining 165 cells.

The procedure adopted for deriving estimated values for grid elements without observational data is similar to that employed in analysis of global heat flow (Chapman and Pollack, 1975; Pollack et al, 1993; Hamza et al, 2008). A variation of this method was considered by Cardoso et al (2010) in which theoretical values of heat flux were derived from the set of coefficients obtained in spherical harmonic expansion of the global heat flux data set. In the present work, we have adopted an updated version of this procedure.

The overall distribution of cells is indicated in Figure 4. The left panel of this figure illustrate distribution of cells, relative to the main age provinces of the continent. A color scheme has been employed for easy visual identification of cells associated with such features as the central cordilleran regions (orange color), pre-cordilleran regions (green color), pre-cordilleran basins (light yellow), intracratonic basins (bright yellow) and Precambrian fold belts and cratonic areas (red). The right panel indicates distribution of cells having observational data (blue dots) and estimated values (red cells).

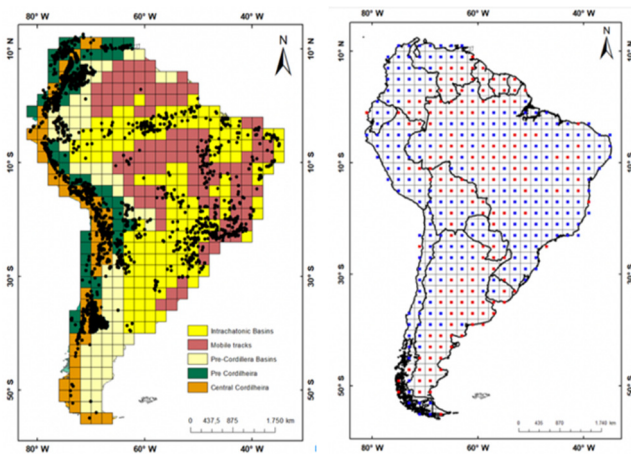


Figure 4 - The left panel indicates  $2^\circ \times 2^\circ$  grid system employed in regional assessments. The right panel indicates distribution of cells with observational data (blue dots) and estimated values (red dots).

## 6. Geothermal gradients and heat flux

The updated data sets were employed in deriving maps of the regional distributions of temperature gradients and heat flux. These are presented respectively in the left and right panels of Figure 5. An examination of this figure reveals that geothermal gradient and heat flux values are systematically high in most of the Andean regions compared to those of the platform areas in the eastern sector. The width of “Andean geothermal belt” is variable. For example, in northern Argentina its width is so large that it extends all the way to the border with Paraguay. Also, there are indications that subsurface thermal field of Patagonian region is different from that of the Brazilian platform in the north.

Another notable feature is the increase in the number of regions with relatively high values of temperature gradients and heat flux, relative to those indicated in the maps of earlier works (Hamza and Munoz, 1996; Hamza et al, 2005; Vieira and Hamza, 2014). This is a consequence of the addition of new values of gradient and heat flux for the volcanic regions, derived using the method of magmatic heat budget (MHB). Also, note the considerable similarities in regional distributions of geothermal gradients and heat flux. The overall pattern observed is, however, similar to those reported in previous works.

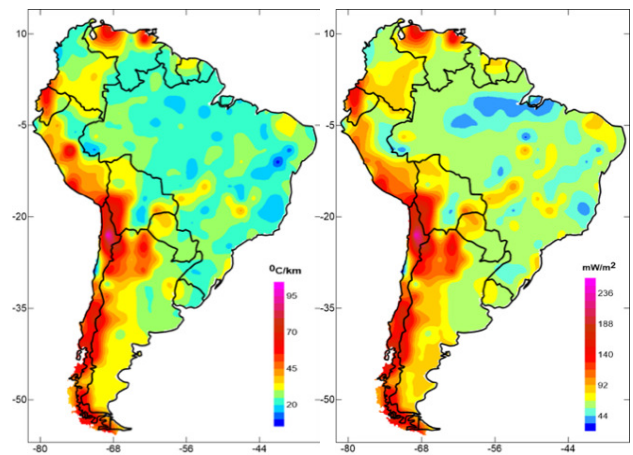


Figure 5 - Regional distributions of geothermal gradients and heat flux in South America.

## 7. Crustal Temperatures

Data sets on heat flux and crustal structure provided the frame work for determining vertical distributions of temperatures in the upper crust. In view of the inherent uncertainties in such data sets, calculations are usually based on simple one-dimensional heat conduction models. These incorporate the effects of depth-dependent variations in thermal conductivity and radiogenic heat production. For layered media with constant thermal properties the relation for temperature ( $T_{zi}$ ) as a function of depth ( $z_i$ ) is (Hamza, 1982):

$$T_{zi} = T_{0i} + \frac{q_{0i} - A_{0i} D_i^2}{\lambda_i} z + \frac{A_{0i} D_i^2}{\lambda_i} [1 - e^{-z_i/D_i}] \quad (4)$$

where  $T_{0i}$  is the surface temperature,  $q_{0i}$  the surface heat flux,  $A_{0i}$  radiogenic heat productivity and  $\lambda_i$  the thermal conductivity of the  $i^{\text{th}}$  element. It is common practice to designate the difference between terms  $T(z)$  and  $T_0$  of equation (4) as the excess temperature ( $\Delta T$ ). The relation for excess temperature is:

$$\Delta T = \frac{q_0}{k} d - \frac{A_0 rad}{2k} \frac{d^2}{k} \left(1 - e^{-z/D}\right) \quad (5)$$

Following the usual practice in geothermal model studies, the value of  $A_0$  is derived from empirical relations (Cermak et al, 1990) relating crustal seismic velocities with radiogenic heat productivity. This model has been employed in the present work for calculating temperature distributions and in deriving maps of basal temperatures of the principal crustal layers. The model calculations were carried out for a set of thermal conductivity values representative of the main regional geologic formations in the continent (Hamza et al, 2005). Such procedures introduce some degree of uncertainty in model results. However, the magnitudes of associated errors are likely to be less than common uncertainties in gradient and heat flux values.

According to results obtained in this work, excess temperatures in the range of 90 to 150°C at depths of one to three kilometers, occur mainly in highlands region of Andean cordillera. These include the volcanic areas as well as regions of occurrences of hydrothermal activities. On the other hand, much lower temperatures occur at similar depths along the eastern parts of the continent. One of the convenient means of illustrating vertical distribution of excess temperatures is by using stacks of crustal temperature maps at conveniently chosen depth levels, allowing a three-dimensional perspective. Results of such an attempt is illustrated in Figure 6, for excess temperatures at depths of 3 to 6 km.

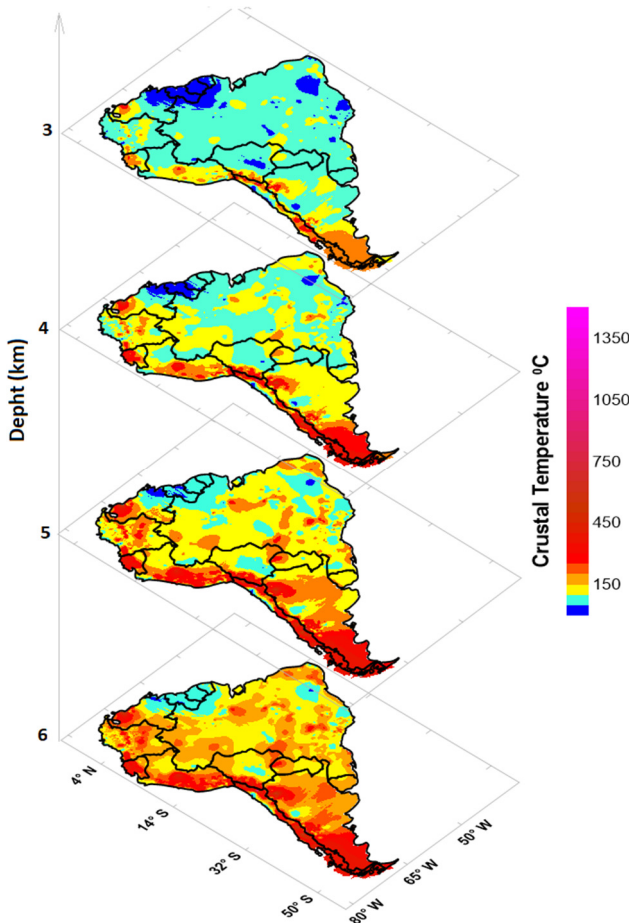


Figure 6 – Stack of maps providing a 3D perspective of crustal temperatures, for depths of 3, 4, 5 and 6 km.

Note that at depths less than 3km occurrences of geothermal systems with temperatures higher than 150°C are limited to the southern volcanic complexes in Chile and Argentina. The possibility that crustal blocks with temperatures higher than 150°C, can be encountered at depths less than 3 km is important for planning exploitation of HDR and HWR systems in these regions.

At larger depth values, of more than 4km, other regions of high temperature systems appear in areas of Altiplano in Bolivia, central Peru, northwestern parts of Ecuador and western parts of Venezuela. The two maps in the lower parts illustrate the distribution of temperatures at the depth range of 5 to 6km. Note that in these cases occurrences of geothermal systems with temperatures higher than 150°C are not limited to the Andean cordilleras. Significantly large high temperature regions extend not only to the eastern sectors of cordilleran regions but also spread out to wide regions in the eastern stable platform areas. Thus, Pre-cordilleran ranges, Chaco and Pampas plains and intracratonic basins in the tectonically stable regions of central Brazil also have temperatures reaching up to 150°C at larger depth levels.

## 8. Resource Estimates

The resource base calculations in the present work were carried out following the methodology proposed in earlier studies (see for example: Muffler and Cataldi (1978), Battocletti (1999), Hutter (2001), Barbier (2002), Cardoso et al (2010). Volumetric method was considered adequate for this purpose. In the terminology proposed by Muffler and Cataldi (1978) the resource base (RB) is considered as the excess thermal energy in the layer up to a specified depth. In gridded data sets the resource base ( $Q_{RBi}$ ) for the  $i^{th}$  cell, of thickness  $d_i$ , associated with the temperature distribution is calculated using the relation:

$$Q_{RBi} = \rho_i C_{pi} A_i d_i (T_i - T_{0i}) \quad (6)$$

where  $\rho_i$  is the average density,  $c_{pi}$  the specific heat,  $A_i$  the area of the cell,  $T_i$  the bottom temperature of the cell and  $T_{0i}$  upper surface temperature.

Recoverable resource (RR) is usually defined as that part of the resource base associated with pore fluids that can be extracted using current technology (see Muffler and Cataldi, 1978; also, Lund and Freeston, 2001). In areas of positive geothermal gradients, temperatures of the rock matrix and the pore fluids increase with depth. However, values of porosity and permeability of most common rocks decrease with depth, which imply a corresponding decrease in quantity of circulating fluids in deeper levels. The nature of opposing roles of temperature and porosity variations with depth can be understood by considering the relation for total geothermal resource ( $Q$ ) of a volume element (of area  $A$  and thickness  $h$ ) with rock temperature  $T_r$  and porosity  $\phi$ :

$$Q = [\phi C_f + (1 - \phi) C_r] [T_r - T_0] A h \quad (7)$$

where  $C_f$  and  $C_r$  are the heat capacities of the fluid and rock matrix respectively. The variation of  $T_r$  with depth  $z$  depends on the local value of geothermal gradient ( $\Gamma$ ). The variation of porosity  $\phi$  with depth  $z$  is usually represented by a relation of the type:

$$\phi = \phi_0 e^{-z/\Pi} \tag{8}$$

where  $\Pi$  is the parameter specifying decrement of porosity with depth. The substitution of Equation (5) in Equation (4) leads to:

$$Q = (z\Gamma Ah)[\phi_0 e^{-z/\Pi} C_f] + (z\Gamma Ah)[(1 - \phi_0 e^{-z/\Pi})C_r] \tag{9}$$

It is fairly simple to note that the first term in equation (9) represents the recoverable resource (RR) while the second term represents the resource associated with the solid rock matrix (RM). The sum of RR and RM represents the resource base (RB). Numerical simulations with representative estimates of the main parameters in Equation (9) indicate that maximum value of recoverable resource occurs in the depth range of 2500 to 3500 meters. Hence, for purposes of the present work, the estimates of resource base and recoverable resources have been set to a reference depth limit of 3 km. Mean values of porosity adopted for the main rock types are 0.25 (soft sediments), 0.15 (hard sediments), 0.1 (fracture zones) and 0.05 (igneous and metamorphic rocks). The estimates of resource base (RB) obtained on the basis of data sets compiled in the present work and using equations (7) and (9) are given in Table 4 for the main countries of South America.

Given in the second and third columns of this table are the surface areas and numbers of localities of data acquisition for each country. The fourth column gives the mean values of the resource base (RB) for each country, expressed in  $10^{21}$  joules. However, it is clear that resource base per unit area (RBUA) is a better indicator of the geographic distribution. Given in the last column of this table are values of RBUA expressed in units of gigajoules per square meter ( $\text{GJ}/\text{m}^2$ ). Countries of the Andean region has RBUA values higher than the overall weighted mean value of  $294\text{GJ}/\text{m}^2$ , the only exception being Colombia. The total number of localities where resources assessments were carried out is 6556. It includes, in addition to 6526 sites of heat flux measurements, 30 localities in British Guiana, French Guiana and Suriname where resource assessments were carried out on the basis of estimated values. Chile stands out as the country with the largest value of RBUA. Significant values of RBUA are also found for Bolivia, Ecuador and Argentina.

As in the case of crustal temperatures it is convenient to illustrate vertical distribution of resource base per unit area by stacking maps at conveniently chosen depth levels. This allows a three-dimensional perspective of resource distribution at different depth levels. Results of such an attempt is illustrated in Figure 7.

Though maps of Figure 7 provide an overall picture of the distribution of resources on continental scale, these are of limited use in providing quantitative information regarding values resources associated with regional blocks. Hence calculations of resources were made for conveniently chosen systems of blocks. In many cases, the boundaries of such regional blocks coincide roughly with those proposed in geologic studies.

An advantage in adopting such classification schemes is that it allows for comparison of resources. In addition, blocks could be chosen in such a way allowing identification of conditions for hosting HDR and HWR resources. In this context, it is convenient explore the relation between

temperature intervals of HDR and HWR systems and the estimates of resources. Results of numerical simulations indicate that values of RBUA greater than  $300\text{GJ}/\text{m}^2$  are associated with temperatures in excess of  $150^\circ\text{C}$  at depths of about 3 km. Hence the localities of such resources may be considered as associated with the presence of HDR type resources at depths pf 3km.

The letter N in the third column of this table refer to the number of estimates. The three-letter codes in the first column of refer to countries where the blocks are situated. The listing in follows the descending order of RBUA values. According to the results of the present compilation 318 sites have potential for developing HDR resources. The errors in resource assessments are estimated to be less than 20%. The weighted mean value of RBUA is  $513\text{GJ}/\text{m}^2$ .

Table 4 - Values of resource base (RB) and resource base per unit area (RBUA) for countries in South America.

Country	Area ( $10^3\text{ km}^2$ )	N	RB ( $10^{21}\text{J}$ )	RBUA* ( $\text{GJ}/\text{m}^2$ )
Chile	760	128	436	577
Bolivia	1100	150	466	425
Ecuador	270	91	113	418
Argentina	2790	436	1146	411
Venezuela	912	40	348	382
Peru	1290	352	431	336
Paraguay	407	35	63	233
Uruguay	178	7	61	224
Colombia	1200	4462	270	223
Brazil	8480	825	1823	215
French Guiana	91	12	13	147
Suriname	163	9	24	146
Guiana	215	9	31	144
Total	17856	6556	5226	294*

\* Indicates weighted mean value.

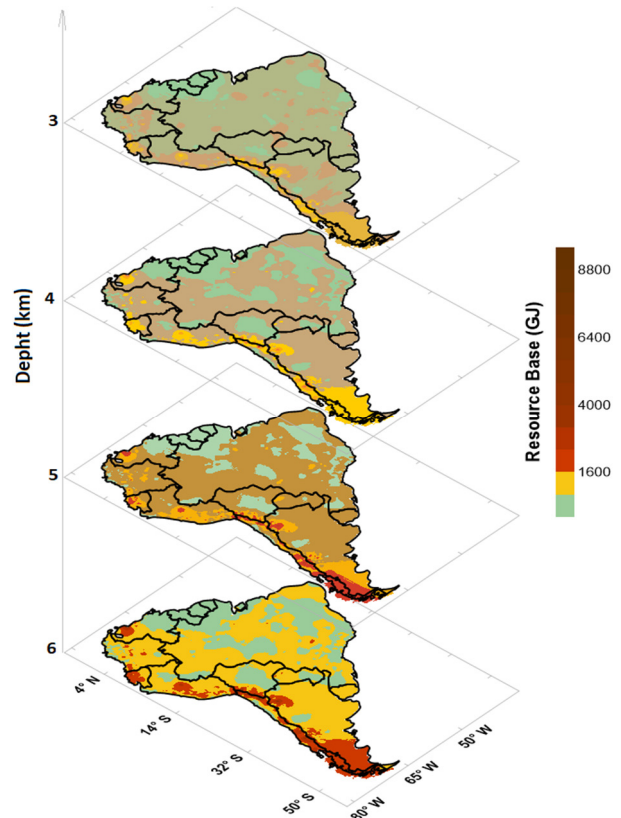


Figure 7 - Stack of maps providing 3D perspective of resource base per unit area (RBUA) for South America, at depth levels of 3, 4, 5 and 6 km.

The resource estimates for French Guiana, Guyana and Suriname are based on estimated values of heat flux. The RBUA values for these countries are the lowest for the south American continent, a consequence of the geological characteristics of cratonic blocks in the northern parts of South America, which imply low heat flux values. Values of RBUA values for countries in the eastern platform areas (Brazil, Paraguay and Uruguay) of the continent are found to be intermediate between those of the western Andean region and the northern cratonic region.

The two maps in the upper parts of this figure illustrate the distribution of RBUA at depths of 3 to 4km. In these cases, occurrences of RBUA with values higher than 500 GJ/m<sup>2</sup> are limited to the southern volcanic complexes in the Cordilleran region, mainly in Chile, Argentina and Bolivia. Other regionally isolated areas of high RBUA occur in volcanic areas of central Peru, northwestern parts of Ecuador and western parts of Venezuela. The two maps in the lower parts illustrate the distribution of RBUA for depths of 5 to 6km. Note that, in these cases, high values of RBUA are limited to the Andean cordilleras.

### 9. Resource Estimates for Regional Settings

Clearly, such resources may be classified as falling into the Hot Dry-Rock (HDR) category. Note that values of RBUA greater than 600 GJ/m<sup>2</sup> are found for five crustal blocks in Chile, one in Peru and another one in Ecuador. RBUA values in the range of 300 to 600 GJ/m<sup>2</sup> occur in three blocks in Argentina, three in Bolivia, two in Chile, one in Ecuador and one in Venezuela.

Results obtained in calculating resource base per unit area (RBUA) are provided in Table 5, for systems inferred to have little fluid contents at shallow crustal levels.

Table 5 - Regions with values of resource base (RB) and resource base per unit area (RBUA), inferred to host HDR type geothermal systems.

Crustal Block	Area	N	RB	RBUA
	(10 <sup>3</sup> km <sup>2</sup> )		(10 <sup>21</sup> J)	(GJ/m <sup>2</sup> )
Principal Cordillera (CHI)	11.8	2	11	909
Western Cordillera (CHI)	35.5	6	28	783
Patagonian Cordillera (CHI)	41.4	7	27	653
Puna Highlands (CHI)	71.0	12	43	612
Central Valley (CHI)	106.0	18	64	601
Puna Highlands (ARG)	83.1	13	438	594
South Volcanic Complex (CHI)	426.0	72	244	574
Central Volcanic Complex (ECU)	95.2	32	52	540
Pri. Cordillera (ARG)	44.7	7	17	433
Altiplano Volcanic Complex (BOL)	403.0	55	194	483
Western Volcanic Complex (ARG)	409.0	64	168	410
South Volcanic Complex (PER)	110.0	30	43	391
Total	1837	318	1329	513*

\* indicate weighted mean value

Similar arguments may also be extended to cases of resources associated with fluid circulation systems in crustal layers. Such resources are better classified as belonging to the category of Hot Wet-Rock systems (HWR). The distinction between HDR and HWR types was made after analysis of the results of hydrogeological studies. There are uncertainties in this procedure, which can be minimized only with further advances in deep crustal studies. Table 6 provides a list of crustal blocks inferred to host significant crustal fluid circulation systems. According to the results of the present compilation 352 sites have potential for developing HWR resources. The total resource base is estimated to be approximately 586x10<sup>21</sup>J. The resource base per unit area 409GJ/m<sup>2</sup>.

There are indications that resources of this type occur in five regions of Peru, three in Venezuela and two in Bolivia. The highest value of RBUA of 692 GJ/m<sup>2</sup> has been found for the site Shanay-Timpishka, situated at the eastern slope of Andean mountains in Peru (Cueto et al, 2016; Ruzo, 2016). This is birthplace of a hot river with temperatures greater than 90°C and discharge rate of >100 m<sup>3</sup>/h. Other similarly high values of RBUA occur in areas of hydrothermal discharges in cordilleran regions of Ecuador and Bolivia. The lowest value found is that for the Pernambuco Lineament (Brazil). In this case where acquisition of conventional geothermal data has not been possible so far, the RBUA values are based on estimates derived from results of magneto-telluric studies. Such results have been interpreted (Santos et al, 2014) as indicative of the presence of a magma intrusion at shallow crustal levels. The structures of this lineament are considered as the westward extension of the Cameroon volcanic chain, in its pre-rift configuration.

Table 6 - Regions with values of resource base (RB) and resource base per unit area (RBUA), greater than 300 GJ/m<sup>2</sup>, inferred to host HWR type geothermal systems.

Crustal Block	Area	N	RB	RBUA
	(10 <sup>3</sup> km <sup>2</sup> )		(10 <sup>21</sup> J)	(GJ/m <sup>2</sup> )
Eastern Slope (PER)	4	1	3	692
Hydrothermal Complex (ECU)	54	18	33	621
Altiplano Hydrothermal Complex (BOL)	315	43	187	594
Chaco Pampas Basin (BOL)	7.3	1	4	491
Falcon Basin (VEN)	23	1	11	482
Central Cordillera (PER)	208	57	82	394
Southern Cordillera (PER)	110	25	36	392
Southeastern Cordillera (PER)	361	99	135	374
Caribbean ranges (VEN)	775	34	7.8	362
Northern Cordillera (PER)	194	53	69	359
Venezuelan Andes (VEN)	114	5	1.14	351
West Pernambuco (BRA)	56.6	15	19.5	344
Total	2221	352	586	409*

\* indicate area-weighted mean value

A careful examination of the regions listed in tables 5 and 6 that there is a close spatial association between the localities of occurrences of HDR and HWR resources. The nature of this relation can be seen in the geographic distributions of the two types geothermal systems, illustrated in Figure 8. The left and right panels of this figure refer respectively to HDR and HWR systems. It appears that in many case HDR resources are present in the core regions of HWR resources.

### 10. Low Enthalpy Resources

Similar approaches have also been employed in assessment of low enthalpy (LE) systems. Since the number of such systems is large it was found convenient to divide these into two groups. The first group consists of systems with temperatures in the range of 60 to 90°C while the second group refer to systems with temperatures in the range 30 to 60°C.

The list of regions that have possibilities for hosting geothermal systems, with RBUA values in the range of 200 to 300 GJ/m<sup>2</sup>, is provided in Table 7.

Table 7 - Estimates of resource base for systems with temperatures of 60 to 90°C.

Region	Area	N	RB	RBUA
	(10 <sup>3</sup> km <sup>2</sup> )		(10 <sup>21</sup> J)	(GJ/m <sup>2</sup> )
Northern Ceara (BRA)	149	22	43.6	293
Southern Goias (BRA)	340	47	97.7	287
Caguan Vaupes Basin (COL)	5.2	19	1.4	272
Putumayo Basin (COL)	54	199	14	264
Llanos Basin (COL)	165	606	43	259
Santa Catarina (BRA)	95	26	24.4	256
State of Sergipe (BRA)	21.9	11	5.6	255
Catatumbo Basin (COL)	115	427	29	252
COR Basin(COL)	22.1	81	5.4	243
Upper Magdalena Basin (COL)	134	492	32	238
Oriente Basin (ECU)	119	40	28	234
Paraguayan Chaco (PAR)	82	35	63	233
Patagonian Uruguay (URG)	271	7	60.8	224
Western parts of Parana (BRA)	150	42	45	226
Mato Grosso do Sul (BRA)	357	8	88	224
Southern Mato Grosso (BRA)	903	32	202	224
Rio Grande do Sul (BR)	282	17	62.8	223
Altiplano / Puna Highlands (PER)	7.3	2	0.073	222
Total	3273	2113	846	240*

\* indicates weighted mean.

A similar case can be made for systems that have temperatures less than 60°C, at depths not exceeding three kilometers. A list of regions that have possibilities for hosting geothermal systems with relatively lower RBUA values are

provided in Table 8. Such systems may be considered as having potential for use of geothermal waters for developing projects with focus on balneology and tourism. According to the results of the present compilation 712 sites have potential for use of geothermal waters in developing agro-industrial projects. The total resource base is estimated to be approximately 848x10<sup>21</sup>J. The high value of RB is a consequence of large areas assigned to LE systems.

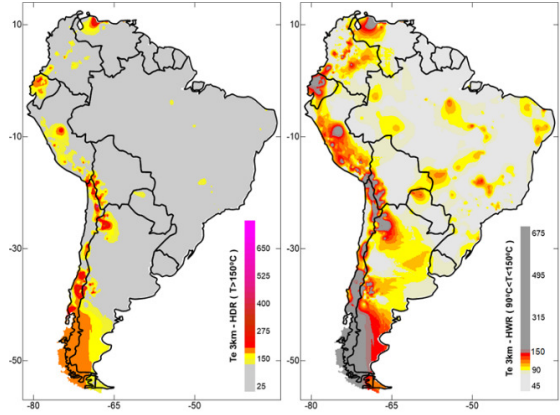


Figure 8 - Geographic distributions of resources associated with HDR (left panel) and HWR (right panel) geothermal systems.

Table 8 - Estimates of resource base for systems with temperatures < 60°C.

Region	Area	N	RB	RBUA
	(10 <sup>3</sup> km <sup>2</sup> )		(10 <sup>21</sup> J)	(GJ/m <sup>2</sup> )
Cesar Rancheria Basin (COL)	1.6	5	0.47	288
EXT basin (COL)	0.8	3	0.23	279
Uraba Basin (COL)	1.1	4	0.2	278
Area NS (COL)	0.5	2	0.13	241
State of Alagoas (BRA)	28	9	6.6	238
Rondonia (BRA)	238	7	56.2	237
State of Roraima (BRA)	224	1	52	232
Eastern parts of the State of Paraiba (BRA)	57	8	12.8	226
State of Parana (BRA)	150	42	45	226
Western parts of Altiplano / Puna (PER)	7.3	2	0.073	222
State of Sao Paulo (BRA)	248	73	54.4	219
State of Tocantins (BRA)	278	38	56	219
Lower Magdalena Basin (COL)	40	145	8	214
Sinu Basin (COL)	12.5	46	2.7	213
Southwestern Minas Gerais (BRA)	587	102	124	211
Western Cordillera (PER)	37	10	0.365	209
State of Maranhao (BRA)	332	38	68.9	208
Guajira Basin (COL)	4.1	15	0.84	205
Total	4188	712	848	212*

\* indicates weighted mean.

The regions listed in Tables 8 should be considered as approximate indications, there being some uncertainty as to the area extent of LE resources with temperatures in the range of 60 to 90°C. Nevertheless, these are inferred to hold potential for low enthalpy (LE) geothermal systems, with use of geothermal waters for developing agro-industrial projects.

As in the case of Table 7 the regions listed in Table 8 should be considered as first-order indications, there being considerable uncertainties in setting limits in the areal extent of LE resources. These are inferred to host low enthalpy (LE) type geothermal systems with potential for developing tourism and balneology facilities.

## 11. Conclusions

The present work constitutes a new look into the nature and distribution of geothermal resources of South America. It is based on recent advances in data analysis and regional assessments. Notable in this context is the progress achieved in the use of a procedure based on magmatic heat budget (MHB) that allow estimation of heat flux in areas of recent volcanic activity. Such advances have allowed resource assessments for 6526 sites, distributed in thirteen countries of the continent. Following this, a 2°x2° grid system with homogenized data ensembles were employed for calculating the in-situ heat content. Determinations of resource base based on observational data are now available for 253 out of a total of 418 cells in this grid system. A summary of resource estimates for geothermal systems in South America is provided in Table 9. Note that occurrences of HDR type resources is limited to fewer number of localities when compared with those of HWR type. As expected, resources of low enthalpy type are present in relatively large number of localities along the eastern parts of the continent.

Table 9 - Summary of resource estimates for geothermal systems in South American continent. RB – Resource base; RBUA – Resource base per unit area; N - number of localities.

Resource Type	T (°C)	N	RB (10 <sup>21</sup> J)	RBUA (GJ/m <sup>2</sup> )
Hot Dry Rock	> 150	318	1329	513
Hot Wet Rock	90 - 150	352	586	409
Low Enthalpy 1 (agro-industry)	60 - 90	3273	240	240
Low Enthalpy 2 (Balneology)	< 60	4188	210	212

Maps based on results of the present work have allowed substantial improvements in assessment of hot dry rock (HDR) and hot wet rock (HWR) resources for several regions. These include tectonically active crustal blocks in southern and central Chile, western Argentina, highland regions of Bolivia, southern parts of Peru, magmatic arcs of Ecuador and cordilleran regions of Colombia and northern Venezuela.

## 12. Acknowledgments

Dr. Mario E. Sigismondi of the University of Buenos Aires provided information on geothermal data of Neuquén basin (Argentina). We thank Dra. Claudia Alfaro of INGEOMINAS (Colombia) for exchange of supplementary information on borehole and oil well temperatures in Colombia.

The second author is recipient of a research scholarship (Process No. 306755/2017-3) granted by the National Research Council of Brazil (CNPq).

## References

- Alexandrino, C., Hamza, V.M., 2018. Terrestrial Heat Flow in Non-thermal ground water circulation settings of Brazil. *International Journal of Terrestrial Heat Flow and Applied Geothermics*, 1(1), 46-51.
- Alfaro, C., Bernal, N., Ramírez, G., Escobar, R., 2000. Colombia: country update. *Proceedings of the World Geothermal Congress*, May 28 - June 10, 2000, Kyushu - Tohoku, Japan, p.45-50.
- Alfaro, C., Alvarado, I., Quintero, W., Hamza, V.M., Vargas, C., Briceño, L.A., 2011. Preliminary map of geothermal gradients in Colombia, *Proceedings of the 12th Colombian Geological Congress*, Paipa (Colombia), p.1-6.
- Almandoz, A.H., Rojas, J.J. 1988. Geothermal Prospects in the Central Region of Sucre State, Venezuela. *Geothermics*, 17, 369-375.
- Almeida, E., 1988. Los Recursos Geotérmicos del Ecuador Continental. Unpublished Interim Report, INECEL (Ecuador).
- Annen, C., Blundy J.D., Sparks R.S.J., 2006. The Genesis of Intermediate and Silicic Magmas in Deep Crustal Hot Zones. *Journal of Petrology*, 47, 505–539.
- Barbier, E., 2002. Geothermal energy technology and current status: an overview. *Renewable and sustainable energy reviews*, 6, 3-65.
- Battocletti, L., 1999. Database of Geothermal Resources in Latin American & the Caribbean. Report for Sandia National Laboratories, Contract No. AS-0989, Bob Lawrence & Associates Inc.
- Beate, B., Salgado, R. 2005. Geothermal country update for Ecuador, 2000–2005. *Proceedings of the World Geothermal Congress*, Antalya, Turkey, 24-29 April.
- Beate, B., Salgado, R. 2010. Geothermal country update for Ecuador, 2005–2010. *Proceedings of the World Geothermal Congress*, Bali, Indonesia, 25-29 April.
- Beck, A.E., 1965. Techniques of measuring heat flow on land. In: Lee, W.H.K., Ed., *Terrestrial Heat Flow*, Monograph No. 8, American Geophysical Union, 24-57.
- Borzotta, E., Caselli, A.T., Mamani, M.J. 2018. Magma Chamber Associated to Deep Faults in Copahue Active Volcanic Complex, South America, Suggested by Magnetotelluric Study. *Geofizicheskiy Zhurnal*, 40, 4. DOI: <https://doi.org/10.24028/gzh.0203-3100.v40i4.2018.140616>.
- Bullard, E.C., 1939. Heat flow in South Africa, *Proc. Roy. Soc. London*, A, 173, 474-502.
- Cardoso, R.R., Hamza, V.M., Alfaro, C., 2010. Geothermal Resource Base for South America: A Continental Perspective. *Proceedings of the World Geothermal Congress*, Bali, Indonesia, 25-29 April 2010.
- Carslaw H.S., Jaeger J.C. 1959. *Conduction of heat in solids*, Clarendon Press, Oxford.

- Carvalho, H.S., Vacquier, V. 1977. Method for determining terrestrial heat flow in oil fields. *Geophysics*, 42, 584-593.
- Cermak, V., Bodri, L., Rybach, L. and Buntebarth, G. 1990. Relationship between seismic velocity and heat production: Comparison of two sets of data and test of validity. *Earth and Planetary Science Letters*, 99, 48–57.
- Chapman, D., Pollack, H. 1975. Global heat flow: a new look. *Earth Planet. Sci. Lett.*, 28, 23–32.
- Cueto, C., Aranda, R.R., Falco Flor, V.G., Saul, F. 2016. “Mayantuyacu Destino Místico”. Unpublished Report, Faculty of Communication Sciences, Technological University of Peru, Lima, Peru, 3 pages. (<http://repositorio.utp.edu.pe/handle/UTP/881>)
- Delgadillo T.Z. 1997. The present situation of geothermal projects in Bolivia (in Spanish). Presented at the Seminar “Development of geothermal resources of latin America and Caribe”. Comisión Económica para América Latina y el Caribe (CEPAL), Santiago del Chile, 10 al 12 de November 1997.
- Diaz H., Guillermo, N. 1988. Potential for developing small geothermal power stations in Peru. *Geothermics*, 17, pp. 381-390.
- Eston, S.M., Hamza, V.M. 1984. Energia Geotérmica no Brasil: Avaliação de Recursos, Avanços Tecnológicos e Perspectivas de Utilização. Simpósio Brasileiro Sobre Técnicas Exploratórias Aplicadas á Geologia, Salvador, 1, 109-132.
- Gomes, A.J.L., Hamza, V.M. 2005. Geothermal gradient and heat flow in the State of Rio de Janeiro. *Revista Brasileira de Geofísica*, 23(4), 325-347.
- Guillier, B., Chatelain, J.-L., Jaillard, E., Yepes, H., Poupinet, G., Fels, J.-F. 2001. Seismological evidence on the geometry of the orogenic system in central-northern Ecuador (South America). *Geophys. Res. Lett.*, 28, 3749-3752.
- Hamza, V.M., Eston, S.M. and Araújo, R.L.C. 1978. Geothermal energy prospects in Brazil: A preliminary analysis. *Pure Appl. Geophys.*, 117, 180-195.
- Hamza, V.M., Eston, S.M. 1983. Assessment of geothermal resources of Brazil – 1981. *Zentralblatt für Geologie und Paläontologie*, 1, 128–155.
- Hamza, V.M. 1982. Thermal structure of the South American continental lithosphere during Archean and Proterozoic. *Rev. Bras. Geoc.*, 12, 149 – 159.
- Hamza, V.M., Frangipani, A., Becker, E.A. 1990. Development of Geothermal Projects in Brazil: Current state and Perspectives. *Proc. International Seminar on Geothermal Perspectives for Latin America and Caribe* (in Spanish), 37-52.
- Hamza, V.M., Muñoz, M. 1996. Heat flow map of South America. *Geothermics* 25 (6), 599–646.
- Hamza, V.M., Gomes, A.J.L. Ferreira, L.E.T. 2005. Status report on geothermal energy developments in Brazil. *Proceedings of the World Geothermal Congress, Antalya, Turkey, 24-29 April.*
- Hamza, V.M., Cardoso, R.R., Gomes, A.J.L., Alexandrino, C.H. 2010. Brazil: Country Update. *Proceedings of the World Geothermal Congress, Bali, Indonesia, 25-29 April.*
- Hamza, V.M.; Verma, R. K. 1969. The relationship of heat flow with age of basement rocks. *Bulletin of Volcanology*, 33, 123-152.
- Hamza, V.M., Cardoso, R.R. and Ponte Neto, C.F. 2008. Spherical harmonic representation of Earth’s conductive heat flow. *International J. Earth Sciences*, 97, 205-226.
- Hurter, S.J. 1986. The use of chemical geothermometry and heat loss models in estimating terrestrial heat flow for low temperature hydrothermal systems. *Rev. Bras. Geofísica*, 6, 33-42.
- Huttrer, G.W. 2001. The status of world geothermal power generation 1995 – 2000, *Geothermics*, 30, 7-27.
- Lahsen, A. 1988. Chilean Geothermal Resources and Their Possible Utilization, *Geothermics*, 17, 401-410.
- Lahsen, A., Sepúlveda, F., Rojas, J., Palacios, C., 2005. Present Status of Geothermal Exploration in Chile, *Proceedings of the World Geothermal Congress, Antalya, Turkey, 24-29 April.*
- Lund, J.W. Freeston, D.H. 2001. World-wide direct uses of geothermal energy 2000, *Geothermics*, 30, 29–68.
- Mamani M.J., Borzotta E, Venencia J.E., Maidana A., Moyano C.E., Castiglione B., 2000. Electric structure of the Copahue Volcano (Neuquén Province, Argentina), from magneto telluric soundings: 1D and 2D modellings. *J. South Am. Earth Sci*, 13,147–156.
- Miranda, F.J., Pesce, A.H. 1997. Argentina Geothermal Resources: New Trends in Development, *GRC Transactions, Volume 21: Meeting the Challenge of Increased Competition*, Davis, CA: Geothermal Resources Council 1997 Annual Meeting, p. 337-339.
- Muffler, L.J.P., Cataldi, R. 1978. Methods for regional assessment of geothermal resources. *Geothermics*, 7, 53-89.
- Murdie R.E., Pugh D.T., Styles P., Muñoz M. 1999. Heat flow, temperature and bathymetry of Lago General Carrera and Lago Cochrane, southern Chile. *Fourth International Symposium on Andean Geodynamics, Göttingen*, 539-542.
- Myers, J.S., 1975. Vertical crustal movements of the Andes in Peru. *Nature* 254, 672-674.
- Noguchi, T., 1970, An attempted evaluation of geothermal energy in Japan, *Geothermics*, 2(pt. 1), 474-477.
- Parodi I.A. 1975. Feasibility of the Development of the Geothermal Energy in Perú—1975. *Lawrence Berkeley Laboratory-Second United Nations Symposium, Berkeley, CA May 1975*, p. 227-231.
- Pesce, A.H. 1995. Argentina Country Update, *Proceedings of the World Geothermal Congress, 1995, Florence, Italy*, p. 35-43.
- Pesce, A.H. 2000. Argentina Country Update, *Proceedings of the World Geothermal Congress, May 28 - June 10, 2000, Kyushu - Tohoku, Japan*, p. 35-43.
- Pesce, A.H. 2005. Argentina Country Update., *Proceedings of the World Geothermal Congress, Antalya, Turkey, 24-29 April 2005.*

- Pollack, H.N., Hurter, S.J. and Johnson, J.R. 1993. Heat flow from the Earth's interior: analysis of the global data set. *Rev. Geophys*, 31, 267–280.
- Rapela, C.W., Pankhurst, R.J., Casquet, C., Baldo, E., Galindo, C., Fanning, C.M., Dahlquist, J.M. 2010. The Western Sierras Pampeanas: Protracted Grenville-age history (1330–1030 Ma) of intra-oceanic arcs, subduction–accretion at continental-edge and AMCG intraplate magmatism. *Journal of South American Earth Sciences*, 29, p. 105-127.
- Ruzo, A. 2016. *The boiling river - Adventure and discovery in the Amazon*. Publisher: Simon & Schuster/ TED (February 2016), 144 pages, ISBN13: 9781501119477.
- Santos, J., Hamza, V.M., Shen, P.Y. 1986. A method for measurement of terrestrial heat flow density in water wells. *Revista Brasileira de Geofísica*, 4, 45-53.
- Santos, A. C. L., Padilha, A. L., Fuck, R.A., Pires, A.C.B., Vitorello, I., Pádua, M.B. 2014. Deep structure of a stretched lithosphere: Magnetotelluric imaging of the southeastern Borborema province, NE Brazil. *Tectonophysics (Amsterdam)*, 610, 39-50.
- Sclater, J.G., Vacquier, V. and Rohrhirsch, J.H. 1970. Terrestrial Heat Flow Measurements on Lake Titicaca, Peru. *Earth and Planetary Science Letters*, 8, 45-54. [http://dx.doi.org/10.1016/0012-821X\(70\)90098-1](http://dx.doi.org/10.1016/0012-821X(70)90098-1)
- Sigismondi, M.E. 2012. Estudio de la deformación litosférica de la cuenca Neuquina: estructura termal, datos de gravedad y sísmica de reflexión. Ph.D. Thesis, Universidad de Buenos Aires, p.1-367.
- Silva, S.L. de., Francis, P.W. 1991. *Volcanoes of the Central Andes*. Berlin Heidelberg New York: Springer. p. 216.
- Smith, R.L., Shaw. H.R. 1975. Igneous-related geothermal Systems, USGS, Cir. 726, 58–83.
- Stern, C. R. 2004 Active Andean volcanism: its geologic and tectonic setting. *Revista Geológica de Chile*, 31(2), 161–206.
- Suarez, T.A. 2017. Cooling of intrusive bodies in the interior of continental crust: effects of the release of latent heat (in Portuguese). Unpublished M.Sc. Thesis, University of Sao Paulo, São Paulo (Brazil).
- Swanberg, C.A., Morgan, P. 1978. The linear relation between temperature based on the silica content of groundwater and regional heat flow: A new heat flow map of the United States. *Pure and Appl. Geophys.*, 117, 227-241.
- Urbani, P.F. 1987. A review of Venezuelan geothermics. *Brazilian Geophysical Journal*, 5, 153-164.
- Vieira, F.P.; Hamza, V.M. 2014. Advances in Assessment of Geothermal Resources of South America. *Natural Resources*, 05, 897-913.